Clinical Cancer Investigation Journal-ISSN: 2278-0513

Evaluation of HSV-1 Effects on Brain Cells Ion Channel Proteins Regulation in HEK293T cells

Abstract

The HSV-1 can use its miRNAs, such as human miRs, to control the expression of ion channels, such as SCN8A, SLC22A2, SLC25A22, and KCNMA1. In this paper, the Target Scan software was used for targeting the ion channel genes by each of the LAT miRs and then two miRs were selected for the continuation of laboratory work. After the development of gene constructs containing each of the miRs and transfecting them into the HEK293T cell line, increased expression of miRs was confirmed by the Real-Time PCR technique, and increased expression of each miR developed by the LAT virus with plasmid transfect containing LAT and H4-5P, H5-5, H7, and H8 miRNAs was evaluated. In the next stage, the target genes were examined. To this end, first, the expression of the genes was evaluated separately using H2 and H3 miRs and based on Real-time PCR reaction. In order to check the effect of LAT transcript on any of the genes, the real-time reaction was performed on cDNAs made by transfection of LAT into HEK293T cells and the Luciferase test was performed on one of the genes (SLC22A2). The results indicate decreased SLC22A2 and SCN8A gene expression as tested by miR-H2 and LAT. As for the two other genes, an increase was observed in their expression, requiring the examination of other upstream and downstream genes. Luciferase assay showed that SLC22A2 is suppressed only by miR-H3, but for confirmation of this finding, it is necessary to check the effect of LAT transcript on SLC22A2. The populations of the study in these channels constitute part of the genes involved in neurological diseases in general and epilepsy in particular. Ionic channels can contribute to epilepsy through mutation or malfunctions, with SCN8A sodium channel playing a major role in such disorders.

Keywords: *Herpes simplex one (HSV-1); Ion channel; Epilepsy; Latency associated transcript (LAT); MicroRNA*

Sarah Mansourabadi, Ehsan Arefian, Zahra Shojaei Jeshvaghani, Bahman zeinali, Masoud Soleimani

[1]*Department of Microbiology, Faculty of Science, University of Tehran, Tehran IRAN*
[2]*Department of Microbiology, Faculty of Science, University of Tehran, Tehran, Iran*
3University Medical Center Utrecht, Netherlands
[4]*Department of cellular and molecular biology, Faculty of Science, University of Tehran, Tehran, Iran.*
[5]*Department of Hematology Tarbiat Modares University, Tehran, Iran.*
**Correspondence author:Sarah Mansourabadi
Email:Sar.mansourabadi@gmail.com

Introduction

Herpes simplex viruses 1 and 2 (HSV-1 and HSV-2) are two members of the herpesvirus family, Herpesviridae, that infect humans. Both HSV-1 and HSV-2 are ubiquitous and contagious. They can be spread when an infected person is producing and shedding the virus. HSV-1 is a neurotropic pathogen associated with painful oral lesions and severe ocular and brain complications. Following infection of sensory neurons, HSV-1 can establish latency and later undergo reactivation in response to various factors, including stress, cold temperature, and skin trauma, resulting in the development of cold sores [1,2]. Viral infection depends on several critical steps including attachment to specific receptors on the host cell membrane and entry and replication of viral genes [2-4]. HSV-1 entry can occur either by direct fusion of the viral envelope with the host cell membrane or by an endocytic mechanism. Although the mechanism (s) by which HSV establishes and reactivates from latency is an area of intense study, much remains unknown. The latency-associated transcript (LAT) RNAs are the only HSV RNAs that have been detected during neuronal latency. LAT has therefore been implicated in latency. LAT produces a family of LAT RNAs including ones of 2, 1.3 to 1.5, and 8.3 kb. After infecting the host, the HSV-1 virus usually lies latent in the trigeminal ganglion. In this situation, the only virus transcript that can be detected in the cell is the latency-associated transcript (LAT). This transcript creates miRNAs that can target the genes and signaling pathways within the cell. On the other hand, given that the virus selects the central nervous system for colonization, it should take advantage of the host cellular facilities, such as ion channels and transporters, which play a key role in the transportation of materials into and out of cells, and development of downstream signaling pathways. According to some studies, these viruses can use ion channels to enter cells and infect them. According to our hypothesis, this virus can use the miRNAs developed by it, such as human miRs, to control the expression of ion channels, such as SCN8A, SLC22A2, SLC25A22, and KCNMA1.

Materials and Methods

The LB medium contains Tryptone and yeast extracts. Tryptone contains amino acids and small peptides, and the yeast extracts supply nitrogen as well as sugars and organic and inorganic materials. The DEMEM medium was used for the culture of HEK293T cells in the presence of FBS. Ampicillin antibiotics were used to select, amplify and purify the plasmid from bacterial cells, and Penicillin and Streptomycin antibiotics were used to develop cell culture media. The DH5α strain was developed using E. coli and HEK 293T eukaryotic cells. Lipofectamine 2000 (Invitrogen) was used for the transfection of genetic structures into the cells. The buffer used for electrophoresis in this study is Tris-acetic buffer. To prepare the buffer, 14.573 g of Tris, 3. 44 ml of % acetic acid,

and 1 .116 g of sodium EDTA were dissolved in 100 ml of water and the pH reached 8. An Antibiotic solution with Stoke concentration (100 mg/ml) was prepared. The final concentration of this antibiotic is 100 µg / ml in the medium. The LAT-associated miRNA sequences of the HSV-1 virus were obtained from the reference and database site. TargetScanCustom software was used to gain access to the target genes of each miRNA.The bacterial host of plasmids carrying both miR-H2 and miR-H3 is E. coli which is a gram-negative bacterium from the Enterobacteriaceae family. DH5α strain was used in the present study. This strain has no RecA enzymes and has therefore lost its genetic recombination capabilities. The two vectors used in this study for the miRs subcloning contain an ampicillin-resistant gene that is developed through a culture of 100 mg of E. coli fluid in liquid broth (LB) medium at an optimum temperature of 37 ° C, at 100 and 120 rpm. The platinum loop is used for flame-sterilized inoculation of solid culture to fluid culture in sterile conditions. The LB medium is prepared by dissolving 2.5 g of LB powder in 100 ml of water. The solution was then sterilized in the autoclave. Once-use sterile plates and LB agar mediums with antibiotics are used for solid culture of E. coli. To prepare this medium, 1.45 grams of agar powder was added to 100 mL of LB medium before autoclaving, and the solution was then autoclaved. After the autoclaved medium cooled down, antibiotics were added to the medium in proportion to the volume of the medium. In order to transfer bacteria from the liquid medium to the solid medium first, an appropriate amount of liquid medium is poured into the middle of the plate and then spread across the sterilized surface utilizing a platinum loop. The vector pCDH-cGFP-Puro was used to express HSV-1-miR-H2 properly. The bacteria carrying each of the pCDH plasmids are pre-cultivated in a small amount of medium containing ampicillin antibiotic. After 12-18 hours of incubation at 37 ° C and appropriate rotation, 10 ml of fluid medium was prepared from each bacteria and incubated overnight. The plasmid in question was extracted from each bacterium according to the plasmid purification kit protocol. This system is based on the alkaline lysis of the bacterium and plasmid binding to the silica gel membrane. The concentration of extracted plasmids is determined with a biophotometer and is electrophoresed on 1% agarose gel to make sure about the purification quality. Using the BamHI and EcoRI enzymes, each of the extracted plasmids is cut according to the figures listed in Table (1).

On the other hand, using the above enzymes, the fragments containing the miR-H2 sequence were isolated from the initial vector pUC57 in a 200 µl enzyme digestion reaction. In order to carry out the enzyme digestion reaction, the tube containing the reactants was stored at 37 ° C for 5 to 6 hours. The reaction product was electrophoresed on agarose gel and the segment in question was extracted and purified using a plasmid purification kit according to the protocol. In the next stage, the final product's concentration was determined, and a small part of it was electrophoresed on agarose gel for verification. Since pUC57 is not an expression vector, we have to look for a final vector to clone the miR-H3 and examine its expression (as is the case for miR-H2). Therefore, vector pCDH-cGFP-Puro was selected. To isolate miR-H3 from the pUC57 vector, we first tried to conduct enzyme digestion using Bam-H1 and EcoR-1 enzymes, but the fragment in question was not isolated due to enzyme problems. Therefore, the PCR method was used to amplify and isolate the miR-H3 fragment with the Pfu enzyme (Table 2). PCR is based on the use of different temperatures at three stages of denaturation, annealing, and extension. A high temperature (usually 94-95 ° C) is used to isolate the strands of the DNA template. Then the temperature is lowered to allow the primers to be annealed to the complementary sequences on the template strings, this temperature depends on the type of primers used. The annealing temperature was set at 60 ° C according to the properties of primers designed in this study. Finally, the temperature is set at the optimum temperature for the DNA Polymerase to produce high-performance DNA. In order to amplify the target DNA, it is necessary to repeat these temperatures in several cycles (25 to 40 cycles). This is done by a thermocycler.

After completion of the PCR reaction, we add 0.25 µg of Taq enzyme to each reaction and place it in the PCR for 72 minutes at 72 ° C to create a *poly*(A) tail. Thus miR-H3 was isolated from the vector pUC-57 and the PCR product was confirmed on the electrophoresis gel. Subsequently, the PCR clean-up kit protocol used for the isolation of primers, enzymes, Mastermix, and other contaminants in the reaction was used as a basis for the purification of the PCR product. In the next stage, the miR-H3 was annealed to the TA vector. To carry out this reaction, the tube containing the reactants was placed at 22 ° C overnight. According to Table 4, the annealing process was performed in a 20µg reaction: The TA ligation product was deactivated for 5 minutes at 70 ° C, and then the calcium chloride method described below was used to produce competent DH5α bacteria and transformed them with the TA-miR-H3 ligation product. Since these vectors are resistant to ampicillin, the culture of the bacteria was carried out in a solid LB medium containing this antibiotic. The quantities used to perform the miR-H2_ pCDH ligation are presented in Table (5). (Primers used here include EF-1-R and CMV-F.)[5-8].

DH5α E. coli was used to carry out the transformation reaction (introduction of vector into bacteria), and the fragments resulting from miR-H3 – TA and miR-H2 – pCDH ligation were separately transformed into this bacterium. The PCR reaction was performed on each of the colonies grown on the

solid LB (antibiotic) medium to confirm the entry of fragments into the E. coli bacterium. The only thing that matters here is the conduction of PCR for 25 cycles to avoid false positive results. Table 6 shows the time cycles of the PCR colony reaction.

Plasmid purification from selected colonies was performed with a plasmid extraction kit to confirm the fragments transformed into bacterial cells. 1% gel is used for the electrophoresis of fragments of the same size as the employed plasmas. 0.15 g of agarose powder was dissolved in 20 ml of TAE solution at the boiling temperature. After cooling the agarose up to the hardening point, it was poured into suitable molds containing electrophoresis combs. The appropriate amounts of DNA samples were mixed with 2 µl of Loading Buffer 6X and poured into each gel well. The electrophoresis time for each sample varies depending on the size of the fragments. After completion of electrophoresis (in TAE 1X buffer at 110 V), flotation in an SYBR SAFE solution was used as a technique for gel staining. After extracting the plasmid from the bacterium containing TA-miR-H3 with the help of the Eco-R1 enzyme, the miR-H3 was isolated from the TA vector according to the reaction presented in Table (7).

After observing the enzyme digestion reaction on the agarose gel and confirming the miR-H3 cuts, the miR-H3 was extracted from the gel using the purification kit and was prepared for ligation to its final vector, i.e. pCDH. To this end, the plasmid backbone is also cut by the Eco-R1 enzyme, but since enzymatic digestion is carried out by a single enzyme, and the self-ligation of the backbone ends is highly probable, it is better to use alkaline phosphatase for treatment before the ligation reaction. However, when a vector is cleaved with a single enzyme or two restriction enzymes with two identical ends (blunt end and Sharp pain such as the enzyme digestion of the xhol and Sall enzymes), the vector DNA should be Dephosphorylated to prevent re-ligation. Table 8 shows the enzymatic reaction of alkaline phosphatase and Table 9 shows the miR-H3 –pCDH ligation reaction [9,10].

A vial of frozen cells kept at -178 ° C (N-tanks) was used to culture HEK 293T cells, The cells were quickly removed from the nitrogen tank and after reaching the ambient temperature in the bin Mari, the cells were moved to a fresh DMEM medium (containing 2mM glutamine and penicillin-streptomycin 1X) and 10% FBS. After centrifugation and discarding the supernatant (until the concentration of the toxic substance DMSO is reduced to zero), the cells were suspended in DMEM medium and 10% FBS and transferred to a 25cm flask. The cells were then incubated at 37 ° C in a CO2 incubator. The growth and status of cells were checked daily since Trypan blue can penetrate the membrane of dead cells and turn them blue, this dye can be used to tally living cells at specific volumes. Various kits are used to extract Total RNA from the cell. The concentration of extracted RNA was measured and was later used for cDNA synthesis based on the transcripts in question. To control the extraction quality, five microliters of RNA extracted on a 1.5% agarose gel prepared under RNase-free conditions, was electrophoresed. The health of ribosomal bands and their strength indicates the power of extraction and the health of the RNAs in question. To determine protein contamination, etc., two microliters of the extraction product were diluted to 100 µl and its absorption at 260 and 280 nm wavelengths was measured, with the absorption ratio of 260 to 280, at best, bringing equal to two. Table 10 shows the materials required for the cDNA synthesis reaction and Table 11 shows the temperatures of the cDNA synthesis reaction [11-13].

Relative Quantification Real-Time P was used to check the quantitative expression of miRNAs and the target genes. SNORD47 and Beta-2m genes were used as reference genes for miRNAs and target genes in HEK cells to normalize the Real-Time PCR results respectively. Cyber Green, I is a double-stranded DNA dye that binds to a small DNA gap and increases the fluorescence power up to one hundred times. However, the PCR reaction can be inhibited at high concentrations. The Real-Time PCR reaction was performed according to Table 12 below.

The Real-time assay of LAT samples was performed by a particular type of primer known as Probe primer designed for each miRNA present in the LAT transcript. To investigate the increased expression of miRs in the LAT transcript, special probe primers were designed for each miR to prevent the primer overlapping effect and false results, Taq man probes which are among hydrolyzer primers designed to enhance the qPCR reaction specificity were used for this purpose. Table 13 shows the essentials of the real-time PCR reaction with the Taq man probe in the ABI device, and Table 14 shows the schedule of the Real-Time PCR reaction process. The Melt process (according to Table 15) was performed on the samples immediately after the PCR reaction

After analyzing the melting curve, the results were reported as cycle thresholds, and the REST 2009 program was used to examine the expression of genes. The Dual-Luciferase Reporter (DLR) Assay was performed to evaluate the reduction in target gene expression. Various vectors have been introduced for this assay. The psiCHECK vector was used in the present study. The enzyme digestion site was used to introduce the target gene sequence into the cloning site, which is located on the ***3′*** regions of the luciferase gene (i.e., along its stop codon). After cloning and obtaining positive results, the resulting vector is transfected into the cell line. Transcription is performed after the fusion of Renilla and the target gene. Luciferase test solutions are prepared in the next stage. 96-well

plates are usually used to perform the Luciferase test. Therefore, first, the cells are transfected with the vector containing the target gene and are observed under a microscope, and then the test is carried out 48 to 72 hours after the transfection. In the next stage, the PLB solution is added to the cell contents depending on the number of wells on the plates. The PLB solution quantities are presented in Table (16).

In order to perform the Luciferase test, the 3'UTR fragments of the target genes were identified using the NCBI site, then the PCR reaction was used to isolate the fragment in question at the appropriate temperature diagram. Then, the fragment in question was amplified in large quantities. The ligation and transformation processes are carried out after the enzyme digestion reaction using the enzymes in the fragment and vector, and finally, we proceed to the next stages if positive results are obtained and sequencing is confirmed. Table 17 shows the materials used in the PCR reaction to isolate the desired 3'UTR fragment referred to as SLC22A2, and Table 18 shows the schedule of the PCR reaction for the isolation of the 3'UTR fragment on the SLC22A2 gene. The type and quantities of materials used in the enzyme digestion of vector psiCHECK (for the final volume of 20 µl) are presented in Table 19.

The vector linearization reaction is performed as presented in Table (19), except that the plasmid quantities vary according to the vector concentration. After that, the fragment and the vector will be ready for the ligation and transformation stages. These stages are described in detail in Table (20):

After the transformation process, the PCR colony reaction was performed on the colonies grown on the plates, and in case the positive colonies and the bands in question were observed, a liquid medium was taken from them, and their plasmids were extracted for the determination of sequences. In the absence of mutation in the binding region of miRNA and the target gene, it was transfected to the HEK293T cell line. 24-well plates were used for this purpose. The remaining steps were carried out as previously mentioned, and the necessary measures were taken for the Luciferase test, the results were reported in the results section.

Results

The results of the bioinformatics search were investigated for ion channels involved in epilepsy targeted with LAT miRs using the TargetScan software, the gene targets involved in the epileptic route, and how they connect, for each of the LAT miRNAs in the HSV-1 virus.

Table 1: The Results of TargetScan analysis

Gene targets involved in epilepsy			**Sequence of seed**	**Name of miRNA**
Connect the seed to the target	Number of target points on 3'UTR	The name of the target genes)(		
7mer	1	SCN8A	CCUGAGC	**miR-H2(3P)**
7mer	1	SLC25A22		
7mer	1	SLC22A2		
7mer-1A	1	KCNMA1	CUGGGAC	**miR-H3(3P)**
7mer-m8 7mer-1A	2	KCNC1	GGUAGAG	**MiR-H4(5P)**
7mer-1A	1	KCNJ10		
8mer	1	SLC25A22	GGGGGGG	**miR-H5(5P)**
8mer 7mer-8a	3	KCNMA1	GGUGGAA	**miR-H7(5P)**
8mer	1	KCTD7		
8mer	1	KCNQ3	UAUAUAG	**miR-H8(5P)**
8mer	1	SLC6A1		
8mer	1	SLC9A6		
7mer-8a	1	GABRB3		

The Targetscan software delivers prediction operations with an emphasis on how the seed of each miRNA is connected and the targeted site's protection level during evolution. In this software, nucleotides 2-7 are defined from the end of the seed adult mRNA5. If the connection is from position 2-8 of miRNA and additionally from position 1 of the nucleotide A target, the connection is reported as 8mer and is in its most powerful situation. If the connection is from the seed position 2-7 of nucleotide 8 participating also in the connection, the connection is reported as 7mer-m8 and when the connection is from the seed position 2-7 and nucleotide 1 is also A, a connection is reported as 7mer-1A. Considering table 21, and according to the importance of all genes targeted by miR-H2 and miR-H3 in the epilepsy disease route and their persistence and expression in the transcript of LAT, thus, it was decided to investigate all genes targeted by them[11-15].

PCDH-cGFP-T2A-puro and pUC57-miR-H3 plasmids were extracted for cloning stages and were taken on the electrophorus gel to correctness of the extraction process.

In figure .2 the obtained band of the pUC57 vector of miR-H3 content shows that it stayed within the range of the 3000 kilobase band. Since miR-H3 isolation was not possible with help of the enzyme digestion directly from the pUC57 vector, we transferred it to vector TA. As said previously, through PCR a piece of about 400 kilobases was isolated that its figure has been shown in figure .3:

After observing the concerned band the product is taken on the gel and then extracted using a clean-up kit. After performing a reaction of connection with TA and the PCR colony reaction, the image of positive colonies is according to figure 4. After observing positive results, we make a plasmid extraction of the group of colonies that had a bolder band and keep the remaining colonies as stock at -70 ° C to be used if necessary. Figure 5 shows the extracted plasmids on the electrophoresis gel with and without enzymatic digestion. As our piece is about 400 base and the vector TA size is about 2729 base, so we have to observe a piece with about 3000 base figures.

In the next stage, the extracted plasmid is cut by Eco-RI limiting enzyme to be prepared for the reaction of connection with the pCDH linear vector. As figure .6 shows, the bold band that stayed up is the undigested vector that is about 3000kilobase and the pale down band is the digested vector. Then with help of extraction kits from the extracted gel and after performing the connection reaction and transformation, the colonies observed on the plate, made the PCR colony reaction, and its result was taken on the electrophoresis gel:

As the miR-H3 is about 400 base and the distance of CMV-F to EF-1R primers is about 200 base, therefore observing pieces 500 to 600 kilobase in figure .7 indicates the correct result. After observation of positive results, the group of colonies having a bolder band is made plasmid extraction, and the remaining colonies also are kept as stock at -70°C to be used if necessary.

In order to perform plasmid transfection LAT in cell stages, we extracted it using a kit whose image is shown on the electrophoresis gel in the figure. 10):

The vector containing LAT-pcDNA3 has a size of about 12 kilobases which is shown in figure .9. The other observed bands in different sizes indicate all products of PCR with SLC22A2 primer gene. For the final confirmation of cloning action and final confidence of the correctness of the cloned sequence, the extracted plasmids of pCDH-cGFP-puro-miR-H2 and miR-H3 pCDH-cGFP-puro were transferred for sequencing. After achieving the results, the obtained sequence was examined with a blast and its correctness was evaluated. Given the incondensable nature of miRNAs, there must be no mutation in their sequence.

In order to examine the performance of the vectors containing these two miRNAs, vectors pCDH-miR-H2 and pCDH-miR-H3 were separately entered into HEK293T cells. Transfection test of HEK 293T cells by vectors, in the case of correct performance considering the GFP protein-encoding gene in vectors, has to be accompanied by the greening of the cells that the vector has entered into them. This is because the green fluorescent protein is green under the fluorescent microscope in green color. Cell transfection for both plasmid groups is made separately in three treatment groups, respectively the first group with a plasmid containing miR-H2, the second group with a plasmid containing miR-H3, and the third group with pCDH backbone plasmid. The third treatment group also can be considered as the backbone control group just contains the gene coding GFP protein. It is while that the first and second treatment groups that are the same recombinant vectors have been made during the project, in addition to having GFP gene containing coding gene of H2 and H3 miRNAs, as well. In addition to the three under-treatment groups, the last groups of the cells were cultured without adding any genetic structure type. In miR-H2 transfection with two repetitions and miR-H3 with two repetitions, the transfection was taken place. In vectors PCDH-cGFP-puro-miR-H2, pCDH-cGFP-puro-miR-H2, miR-H2, and miR-H3 are expressed under CMV promoter and copGFP protein under promoter EF1. in the case performing transfection correctly and entering vectors into cells and also the proper performance of promoters, the transfected cells will be seen in green color under a fluorescent microscope. On the other hand, in the untreated group, given the lack of adding any vectors, the cells haven’t become green.

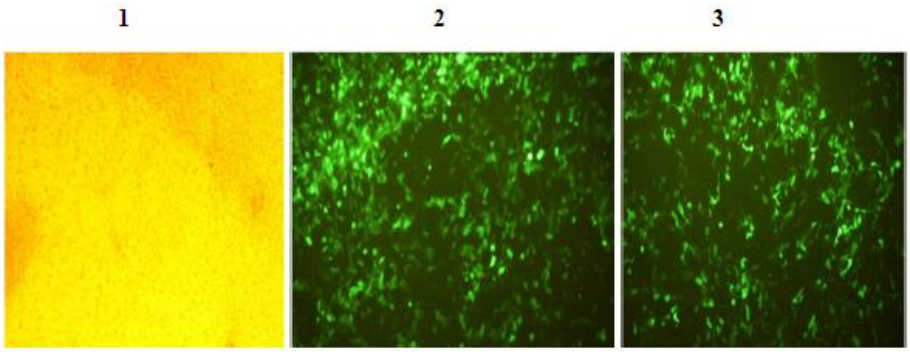

a) Results of cell transfection with pCDH-cGFP-Puro-mir-H2. Figure 1. Images of cells under an optical microscope and figures 2 and 3 show 24 and 48 hours after transfection under a fluorescent microscope, respectively.

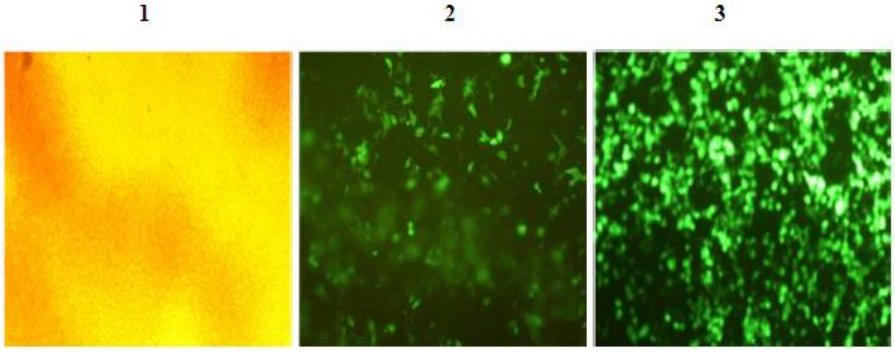

b) Results of cell transfection with pCDH-cGFP-Puro-mir-H3. Figure 1: cells under an optical microscope and figures 2 and 3 show 24 and 48 hours after transfection under a fluorescent microscope, respectively.

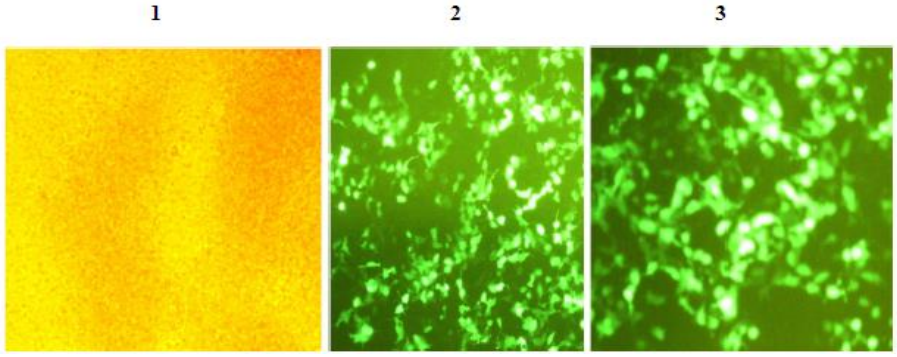

c) Results of cell transfection with pCDH-cGFP-Puro. Figure 1. Images of cells under an optical microscope and figures 2 and 3 show 24 and 48 hours after transfection under a fluorescent microscope, respectively.

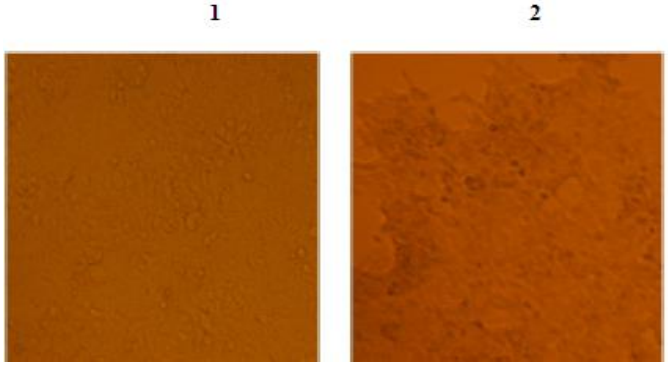

Figure .15. HEK 293T cells, 24 and 48 hours after transfection with miR-H2 and miR-H3 vectors

a) Cells transfected by pCDNA-3-LAT in figures 1 and 2 show 24 and 48 hours after transfection, respectively. (the reason for the color of the image is the lack of a GFP reporter marker).

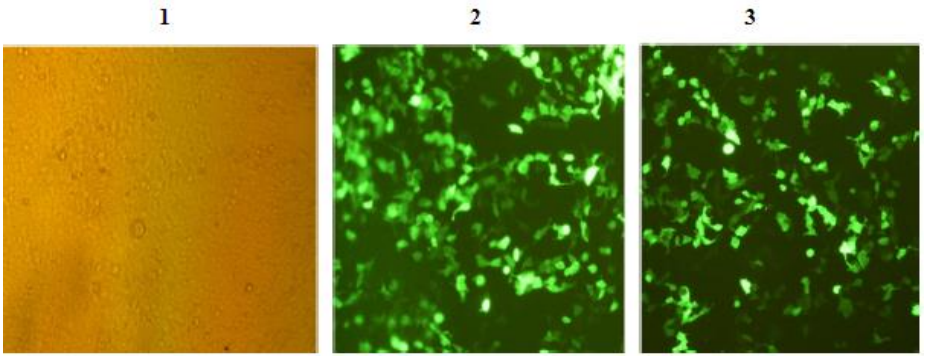

b) Cells transfected with the pCDH-cGFP-Puro-miR-H2 vector in figure 1, respectively including optical microscope, and Figures 2 and 3 show 24 and 48 hours after transfection by fluorescent microscope.

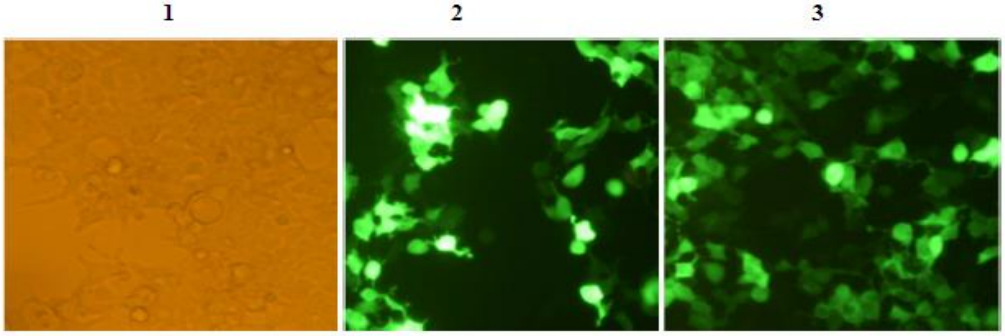

c) Cell transfected with pCDH-cGFP-Puro-miR-H3 vector in figure 1, respectively including optical microscope, and figure 2 and 3 show 24 and 48 hours after transfection by fluorescent microscope.

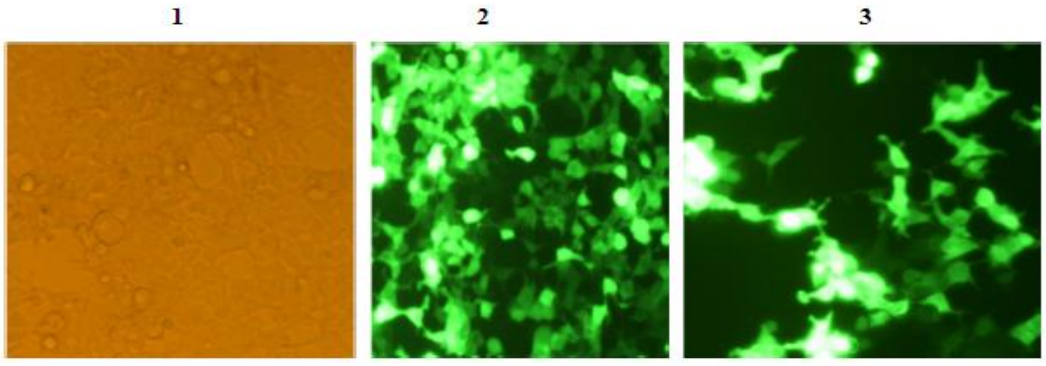

d) Cell transfected with pCDH-cGFP-Puro-miR-H4 vector in figure 1, respectively including optical microscope, and figure 2 and 3 show 24 and 48 hours after transfection by fluorescent microscope.

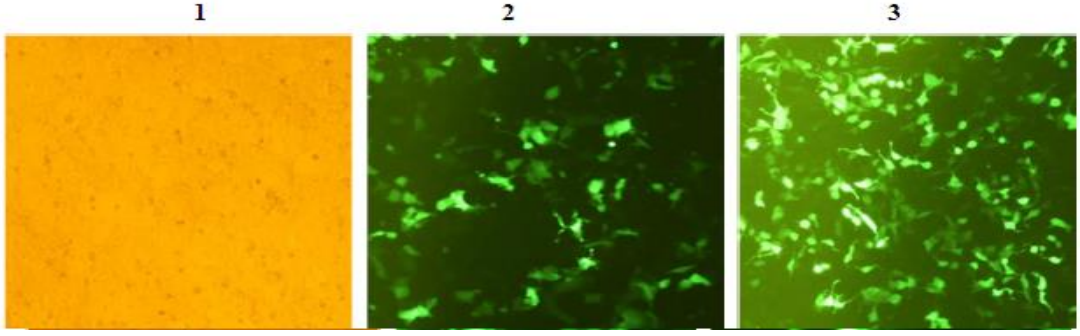

e) Cell transfected with pLEX-jRed-Puro-miR-H7 vector in figure 1, respectively including optical microscope and figure 2 and 3 show 24 and 48 hours after transfection by fluorescent microscope.

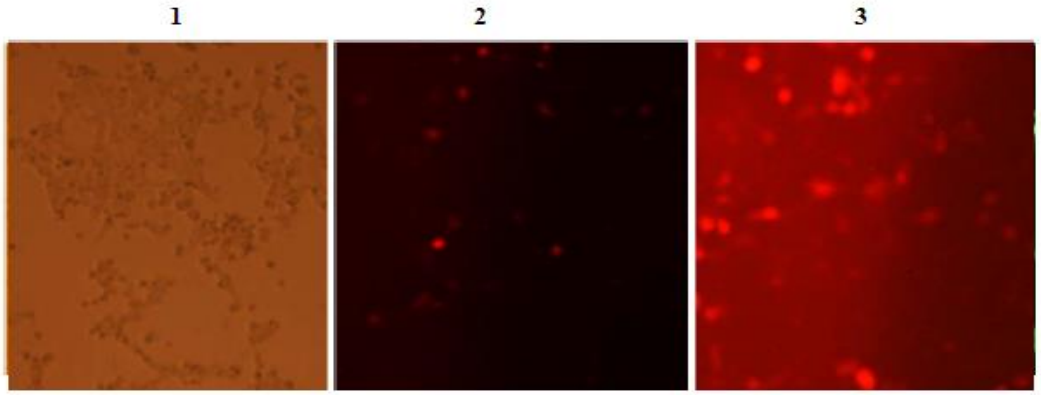

f) Cell transfected with pLenti-III-EGFP -miR-H8 vector in figure 1, respectively including optical microscope, and figure 2 and 3 show 24 and 48 hours after transfection by fluorescent microscope. The reason for the red color is the presence of the jRed reporter.

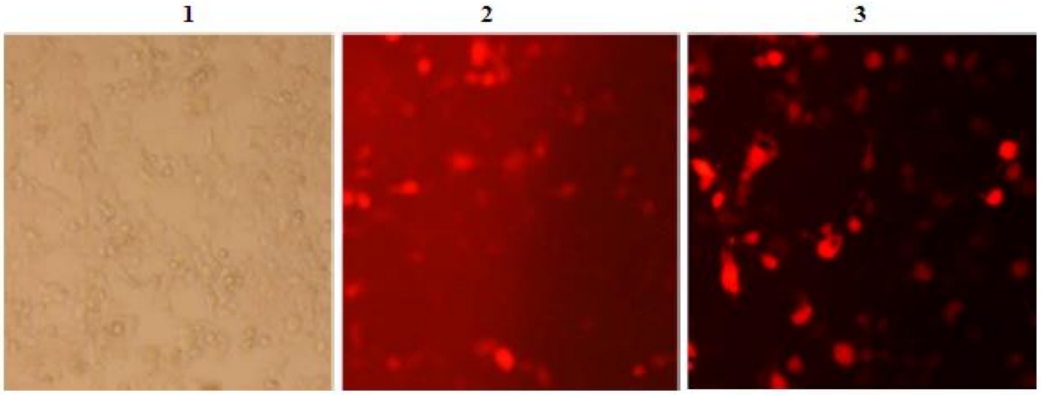

g) Cell transfected with pLenti-III-EGFP vector in figure 1, respectively including optical microscope and figure 2 and 3 shows 24 and 48 hours after transfection by fluorescent microscope.

Figure .16. Results of HEK293T cells transfection with vectors containing LAT transcript and the set of miRs originated from it

The important parameter in analyzing Real-time PCR data is a parameter called threshold cycle. This threshold shows the cycle in which all samples in the analysis have entered into the logarithmic phase and in the ideal mode that primer has optimum efficiency in each stage PCR products are doubled. After determining the threshold line the component of the length of the confluence of this line with each of the fluorescent vectors will suggest the related cycle. This stage of the Real-time PCR data analysis was performed in Stepone software v2.3. After achieving the data concerning the threshold cycle, these data were entered into Rest 2009[1] program to analyze expression rate and statistic evaluations. This program is a product of QIAGEN Company and is applicable for analyzing data resulting from Real-time PCR.

Expression of miRNAs H2 and H3 and also LAT transcript and other miRNAs of the virus, in the cells transfected with plasmids containing each of these miRNAs, was examined by analyzing Real-time PCR data. From the transfected cells containing backbone plasmid pCDH and in the last stage of cell transfection simultaneously all miRNAs every post simplex one by one with LAT transcript were entered into Petri cells together, and pLenti-puro that has no miRNA was used as control. Results concerning the quantitative expression of each miRNA compared to the quantitative expression of Snord47 were normalized as an internal control. The internal control genes must have a relatively stable expression within cells. It is assumed that the expression of these genes doesn't change in the effect of treatment. For this reason, by assuming the stability of control genes expression, this expression can be used as a criterion to compare the difference rate in the two groups. Table 22, shows the rate of miRNAs expression in the treatment groups compared to backbone control pCDH. As can be observed the rate of HSV-1-miR-H2 and HSV-1-miR-H3 expression in the treatment groups with related vectors compared to the treatment group of pCDH backbone vector has enhanced and shows expression increase. Also, results from the analysis performed by Rest software are observed in the figure. 17 through the diagram.

[1] Relative expression software tool

Table 22. results of a statistical examination of data of miRNAs expression in HEK293T treatment groups compared to the control group

Expression	Gene	Gene type	Expression	Std.Error	P-value	Result
miRNA	snord	Internal	1		-	-
	HSV-1-miR-H2	Target	328.557	2.883-3388.87	<0.05	enhancement
	HSV-1-miR-H3	Target	136.712	121.927-154.54	<0.05	enhancement

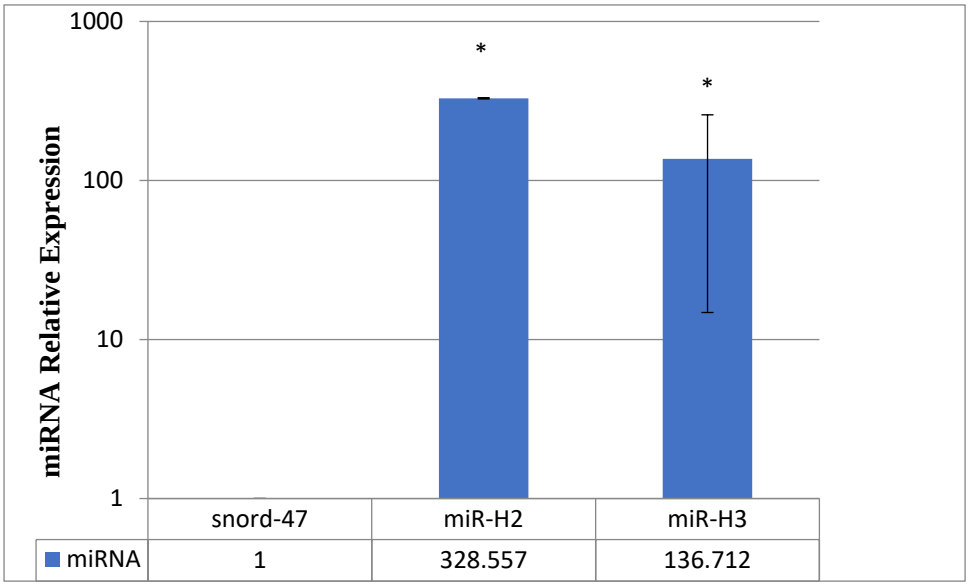

Figure .17. Results of examining statistical data of miR-H2 and miR-H3 expression rate in the treatment group concerning backbone in HEK293T cells.

Starred diagrams imply the significance of the results. Accordingly, miR-H2 and miR-H3 have become 328 and 136 times more, respectively, and this indicates that they have had an expression increase in cells HEK. The marked bars in the diagram are a dispersion of data from qPCR.

Of course, it has to be mentioned that mil bars observed in diagram 17 and the other diagrams wouldn't indicate standard error of data, but are a matrix of real-time data dispersion that has been displayed in the diagram in the form of black lines. In fact, this kind of diagram isn't appropriate to display descriptive data. Particularly they are used for statistical populations. In this case, the most suitable way to exhibit results is using a box or whisker chart in which the median parameter is used so that erroneous data and outliers wouldn't interrupt the general analysis statistically. Figure .18 shows the curve of melting in Real-time PCR analysis of each H2 and H3 miRNA and also Snord 47 in the HEK293T transfected cells. As is observed in each curve, the picks related to all reactions are coincided and take place at a single temperature. Also, in the control samples that lack cDNA or no pick wasn't observed or picks were nonspecific and related to dimmer-primer formation. These observations indicate the high accuracy of the analysis and confirm its results. In figure .19 also proliferation curves concerning each of the miRNAs have been presented.

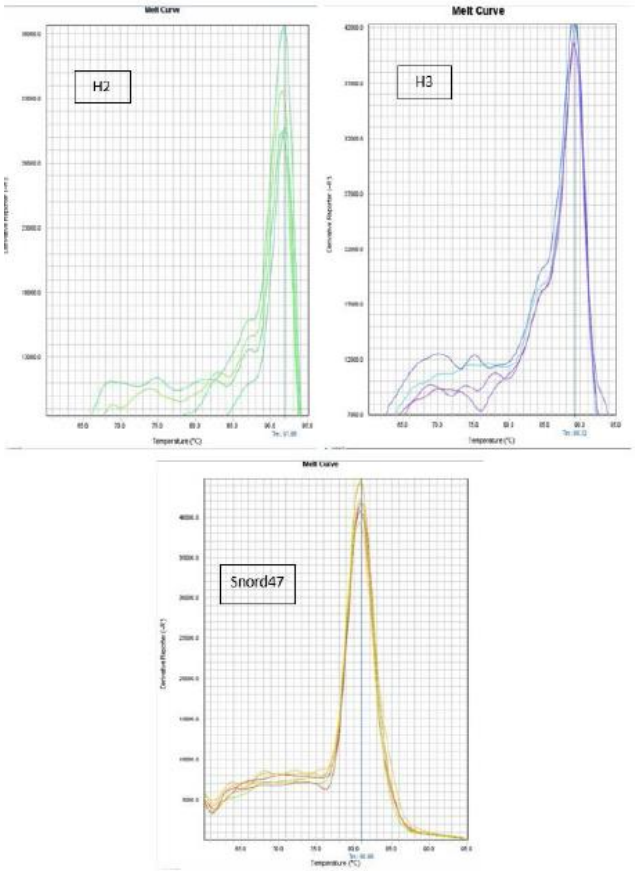

Figure .18. curve of melting miR-H2, miR-H3 and Snord-47 in analysis Real-time PCR in HEK293T cells

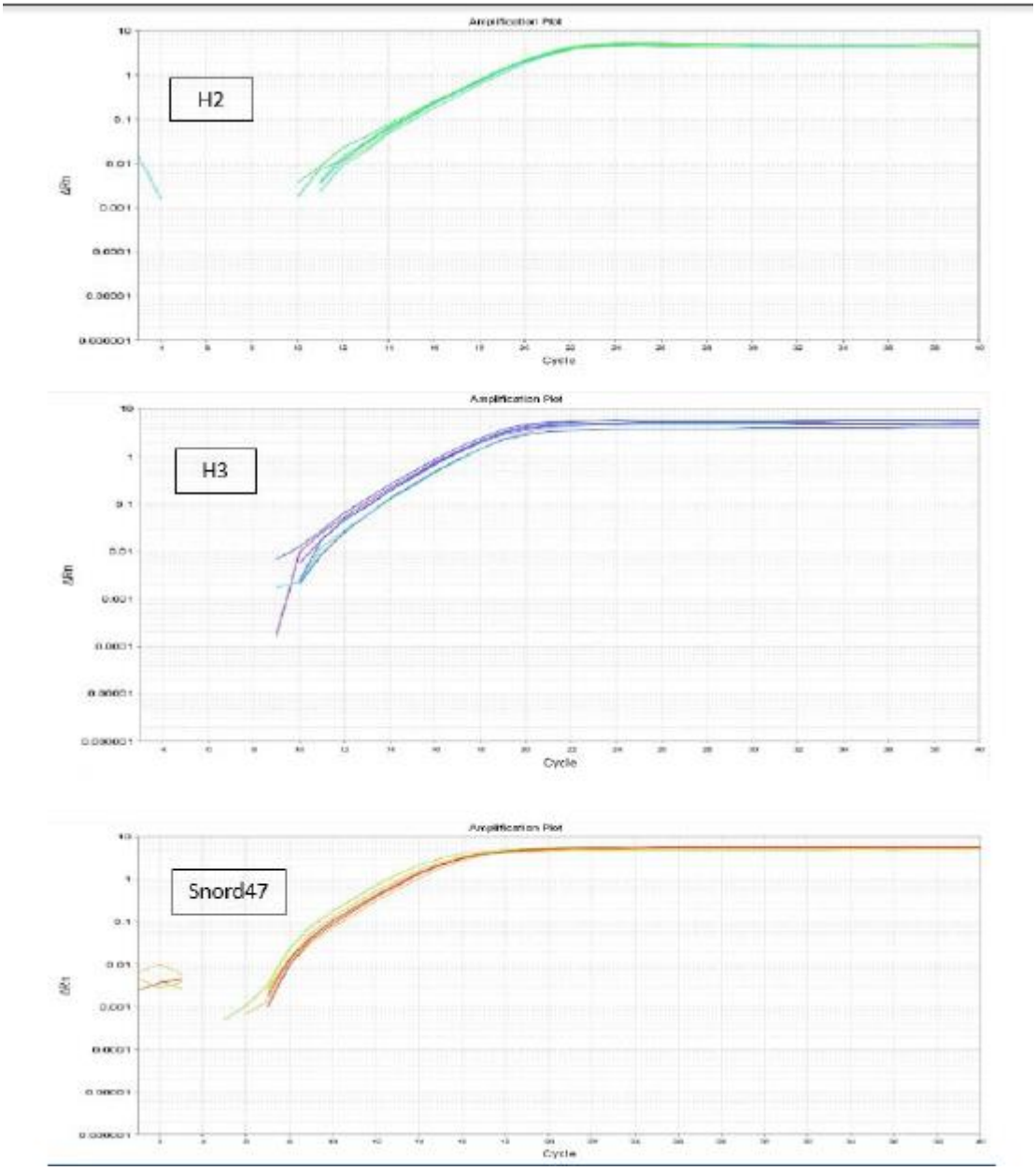

Figure .19. Proliferation curve of piece miR-H2, miR-H3, and Snord-47 in the HEK293T transfected cells.

Now that a significant expression increase of miRNAs was ensured in the treatment groups, in the next step, the impact of this expression increases on ionic channel genes can be examined. Considering the predicted gene targets for each of H2 and H3 miRNAs through Target Scan software, Table 21, and their available possibilities, the selected genes include SCN8A ،SLC22A2 ،SLC25A22 ،KCNMA1.

Using Total DNA synthesized from TNA extracted from each treatment group, the possibility of Real-time PCR analysis is provided for each of the above genes in the treatment and control groups. To normalize each gene, the B2M gene was used as an internal control. Tables 23 and 24 show expression changes of each target gene respectively in the transfected groups with vectors bearing miR-H2 and miR-H3 compared to the control group transfected with backbone vector (pCDH), respectively.

Table 23. Results of statistical surveys of targeted genes expression in the groups treated by miR-H2 compared to the control group in HEK293T cell

Gene	Gene type	Expression	Std. Error	p-value	Result
Beta-2M	Internal control	1		-	-
SCN8A	Target	0.056	0.006-0.402	<0.05	**Reduction of expression**

SLC22A2	Target	0.01	0.001-0.152	0.05<	**Reduction of expression**
SLC25A22	Target	0.309	0.257-0.304	<0.05	**Reduction of expression**

Table 24. Results of statistical surveys of targeted genes expression in the groups treated by miR-H3 compared to the control group in HEK293T cell

Gene	Gene type	Expression	Std. Error	p-value	Result
B2M	Internal control	1		-	-
KCNMA1	Target	24.847	16.895-6.585	0.05<	**Increase expression**

Also, results from the analyses performed by Rest2009 software in figure 21 are shown in the diagram.

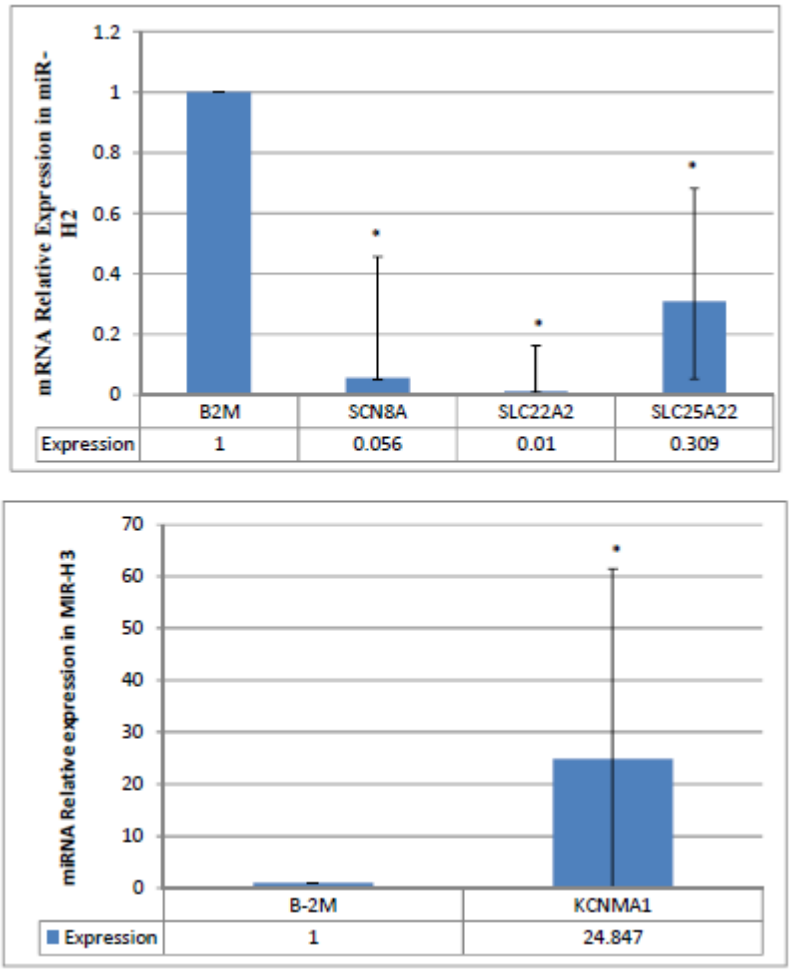

Figure .20 Statistical results of targeted genes expression in the groups treated by miR-H2 and miR-H3

The up figure is the statistical results of target genes affected by miR-H2 and the down figure is the statistical results of target genes affected by miR-H3 (star, implies the significance of decrease or increase of gene expression). As it is obvious genes SCN8A، SLC22A2 and SLC25A22 all in the effect of miR-H2 have undergone expression decrease. In the opposite result only the target gene of miR-H3, KCMNA1, has increased strongly.

Table 25. Rate of miRNAs expression compared to a control group of backbone in LAT transcript

Gene	Gene type	Expression	Std. Error	p-value	Result
Snord-47	Internal control	1		-	-

miR-H2	Target	621688	67.002-11188.901	<0.05	**Increase expression**
miR-H3	Target	10.611	2.815-30.193	<0.05	**Increase expression**
miR-H4-5P	Target	337209	10.943-11474.619	<0.05	**Increase expression**
miR-H5	Target	573455	387.414-952.361	<0.05	**Increase expression**
miR-H7	Target	6.989	5.372-9.355	<0.05	**Increase expression**
miR-H8	Target	5.355	3.207-8.886	>0.05	**meaningless**

As it is obvious, all miRs expression rate in the groups treated by them has enhanced backbone vector. As LAT is a transcript of all miRs, then this increase in their expression is expectable.

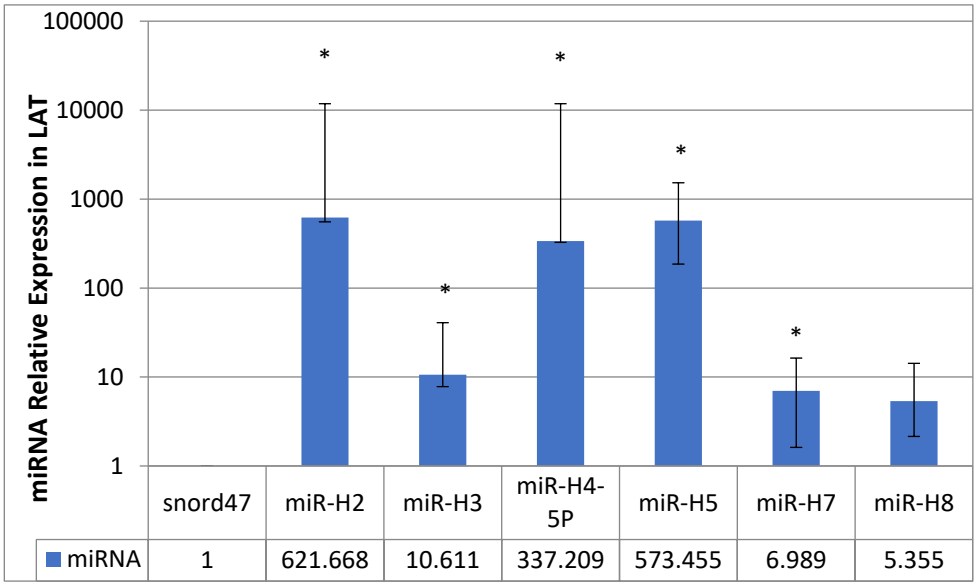

Figure .21. Results of statistical surveys of miRNAs expression data in treatment groups compared to backbone group in the LAT transcript in HEK293T cells

As it is obvious all miRs existing in LAT particularly H2, H4, and H5 miRs have had an increase in expression (starred indicator implies the significance of expression increase). Of course, this rate of expression increases in H2, H4, and H5 miRs have taken place to a more extent. Table 26 Results of statistical surveys of the expression data of the target genes miR-H2 and miR-H3 in treatment groups compared to the backbone group affected by LAT in HEK293 cells

Gene	Gene type	Expression	Std. Error	p-value	Result
B2-M	Internal control	1		-	-
SCN8A	Target	0.029	0-8.731	0.05<	**Reduction of expression**
SLC22A2	Target	0.282	0.049-1.3	0.05>	**meaningless**
SLC25A22	Target	3.655	2.997-4.473	<0.05	**Increase expression**
KCNMA1	Target	33.104	22.517-49.16	<0.05	**Increase expression**

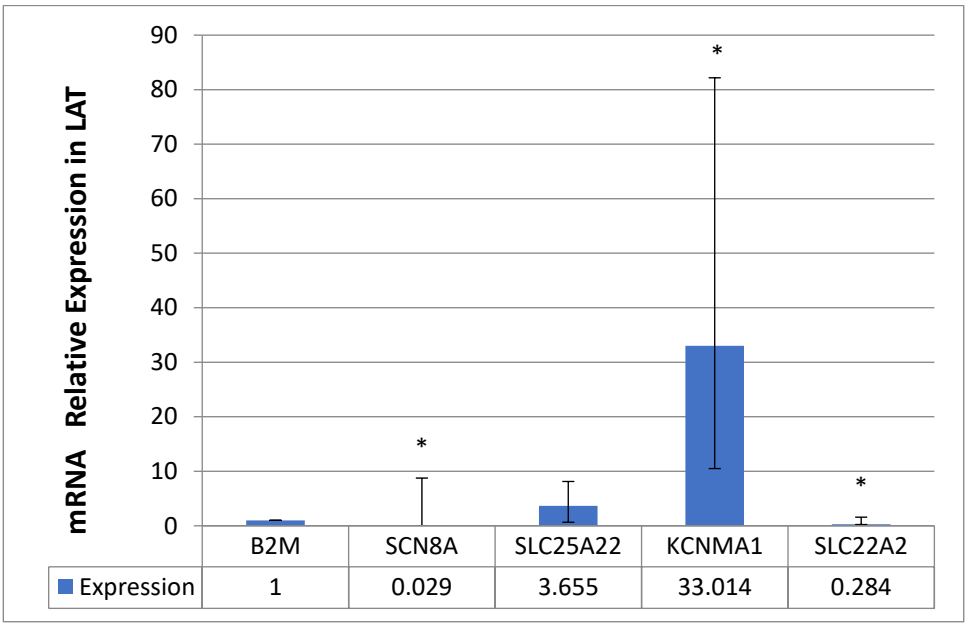

Figure .22 Results of statistical surveys of expression data of mRNAs in treatment groups compared to backbone group in LAT transcript in HEK293T cells

According to the figure.22 diagram and obtained data, SCN8A and SLC22A2 genes affected by LAT have had expression decrease but SLC25A22 and KCNMA1genes have had expression increase. Although this reduction isn't significant regarding SCN8A and SLC22A2 genes, because these types of diagrams are suggested based on descriptive data, only can show obtained data dispersion. We have investigated the impact of the miRs expression in HEK293T cells separately and its results have been presented in table 27.

Table 27. Results of study of miR-H4-5P، H7 and H8 expression in HEK293T cells

Gene	Gene type	Expression	Std. Error	p-value	Result
Snord47	Internal control	1		-	-
miR-H4-5P	Target	2787.27	2176.22-3659.43	0.05<	**Increase expression**
miR-H7	Target	311.05	236.676-415.914	<0.05	**Increase expression**
miR-H8	Target	1.345	1.19-1.521	<0.05	**Increase expression**

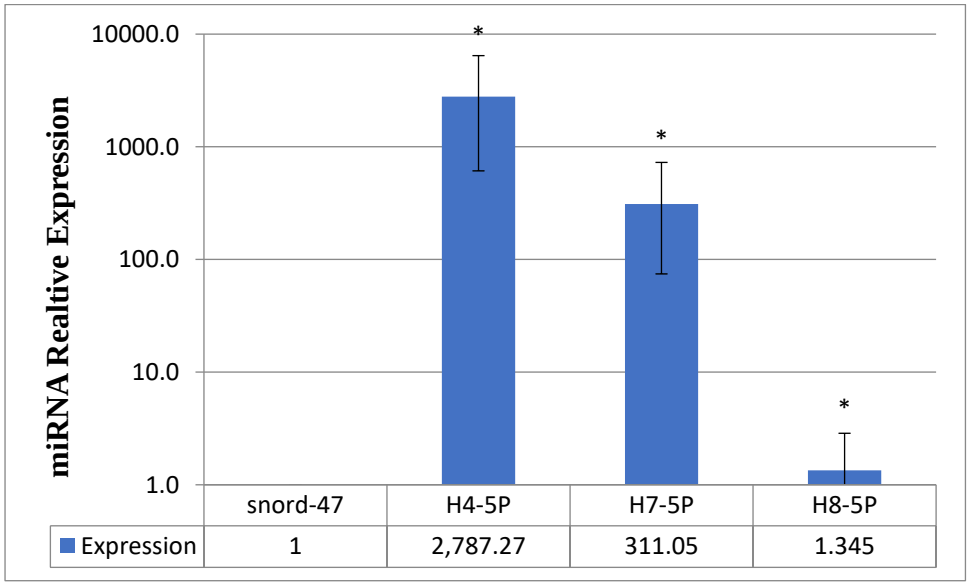

Figure.23. Results of study of miR-H4-5P، miR-H7 and miR-H8 expression in HEK293T cells

Table 28. Statistical data of target genes expression affected by miR-H2

Gene	Gene type	Expression	Std. Error	p-value	Result
B2-M	Internal control	1		-	-
SCN8A	Target	0.056	0.006-0.402	>0.05	**Meaningless**
SLC25A22	Target	0.93	2.997-4.473	>0.05	**Meaningless**
KCNMA1	Target	0.883	0.6-1.304	>0.05	**Meaningless**

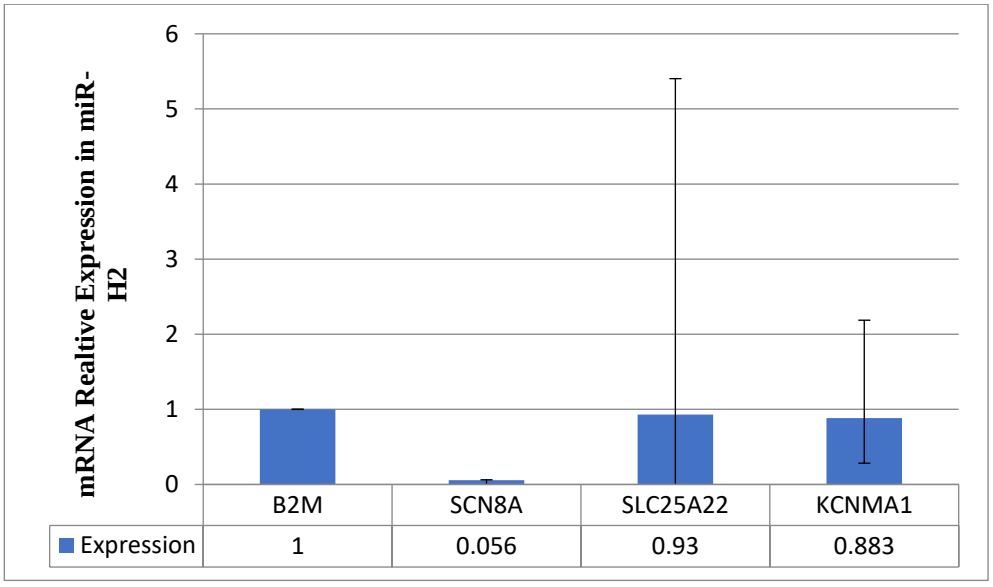

Figure 24. Results of statistical surveys of mRNAs expression data targeted in miR-H2 compared to backbone group (pLenti-III) in HEK293T cells

As figure .24 shows the effect of miR-H2 on its direct target genes is decreasing effect and on the KCNMA1 gene which has been introduced as a direct target of miR-H3, is increasing effect. However, its reduction isn't significant in terms of Rest analysis.

Table 29. Statistical data of target genes expression affected by miR-H3

Gene	Gene type	Expression	Std. Error	p-value	Result
B2-M	Internal control	1		-	-
SCN8A	Target	5.169	4.625-5.818	0.05<	**Increase expression**
SLC25A22	Target	3.138	2.577-3.861	<0.05	**Increase expression**
KCNMA1	Target	24.847	16.895-35.585	<0.05	**Increase expression**

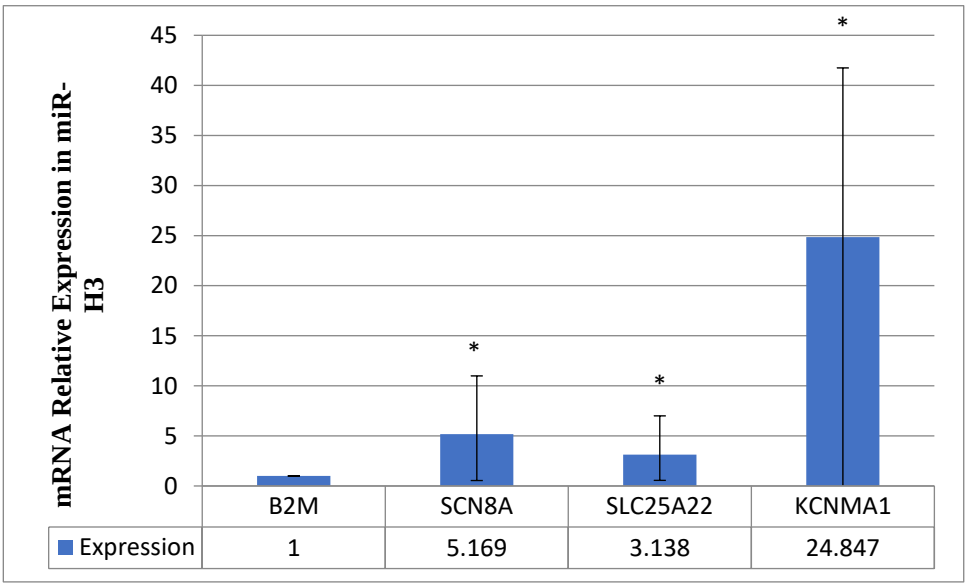

Figure 25. Results of statistical surveys of mRNAs expression data targeted in miR-H3 compared to backbone group (pLenti-III) in HEK293T cells

As figure 25 shows the effect of miR-H3 on the direct target genes of miR-H2 namely SCN8A and SLC25A22 is increasing effect and on the KCNMA1 gene that has been introduced as a direct target of miR-H3, is also increasing effect.

Table 30. Statistical data of the target genes expression affected by the miRNA set existing in miR-H4

Gene	Gene type	Expression	Std. Error	p-value	Result
B2-M	Internal control	1		-	-
SCN8A	Target	11.236	9.328-13.701	0.05<	**Increase expression**
SLC25A22	Target	12.084	9.91-14.805	<0.05	**Increase expression**
KCNMA1	Target	20.832	14.243-31.183	<0.05	**Increase expression**

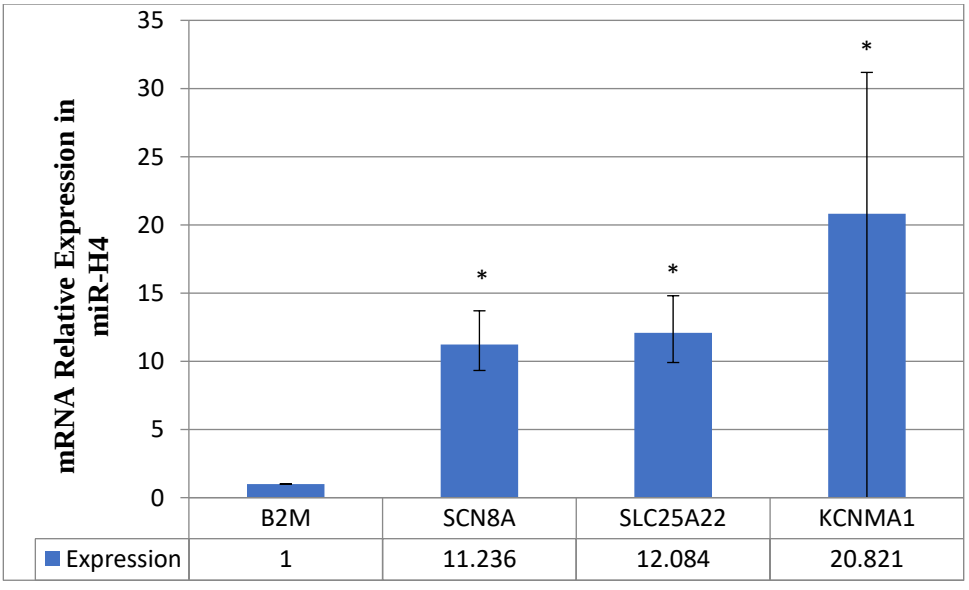

Figure 26. Results of statistical surveys of mRNAs expression data targeted in miR-H4 compared to backbone group (pLenti-III) in HEK293T cells

As figure 26 shows the effect of miR-H4 on the direct target genes of miR-H2 namely SCN8A and SLC25A22 is increasing effect and on the KCNMA1 gene that has been introduced as a direct target of miR-H3, is also increasing effect.

Table 31. Statistical data of the target genes expression affected by the miRNA set existing in miR-H7

Gene	Gene type	Expression	Std. Error	p-value	Result
B2-M	Internal control	1		-	-
SCN8A	Target	5.704	4.994-7.705	0.05<	**Increase expression**
SLC25A22	Target	2.302	0.89-3.459	<0.05	**Increase expression**
KCNMA1	Target	10.111	8.88-15.75	<0.05	**Increase expression**

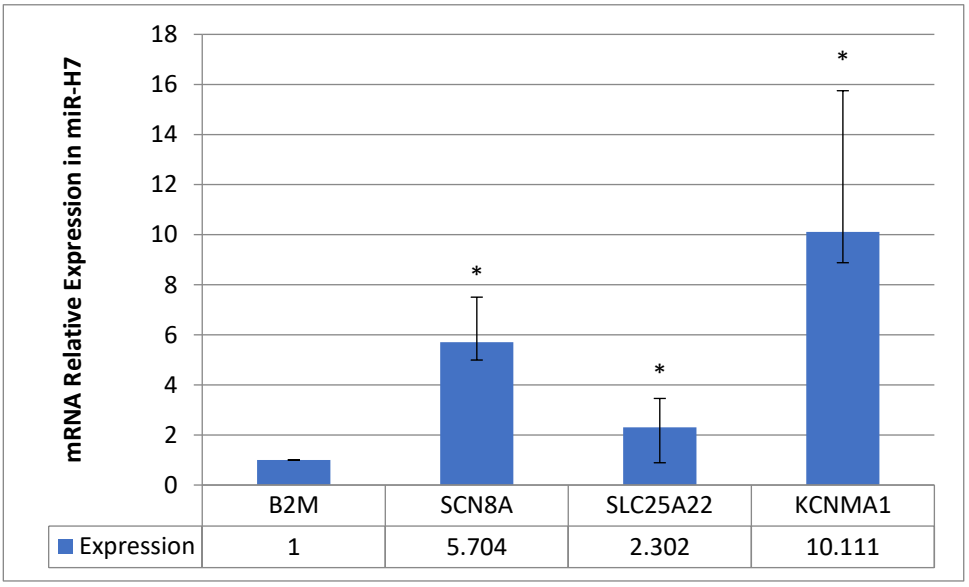

Figure 27. Results of statistical surveys of mRNAs expression data targeted in miR-H7 compared to backbone group (pLenti-III) in HEK293T cells.

As figure 27 shows the effect of miR-H7 on the direct target genes of miR-H2 namely SCN8A and SLC25A22 is increasing effect and on the KCNMA1 gene that has been introduced as a direct target of miR-H3, is also increasing effect.

Table 32. Statistical data of the target genes expression affected by the miRNA set existing in miR-H8

Gene	Gene type	Expression	Std. Error	p-value	Result
B2-M	Internal control	1		-	-
SCN8A	Target	6.704	5.994-7.505	0.05<	**Increase expression**
SLC25A22	Target	2.007	1.646-2.459	>0.05	**meaningless**
KCNMA1	Target	13.132	9.009-19.768	<0.05	**Increase expression**

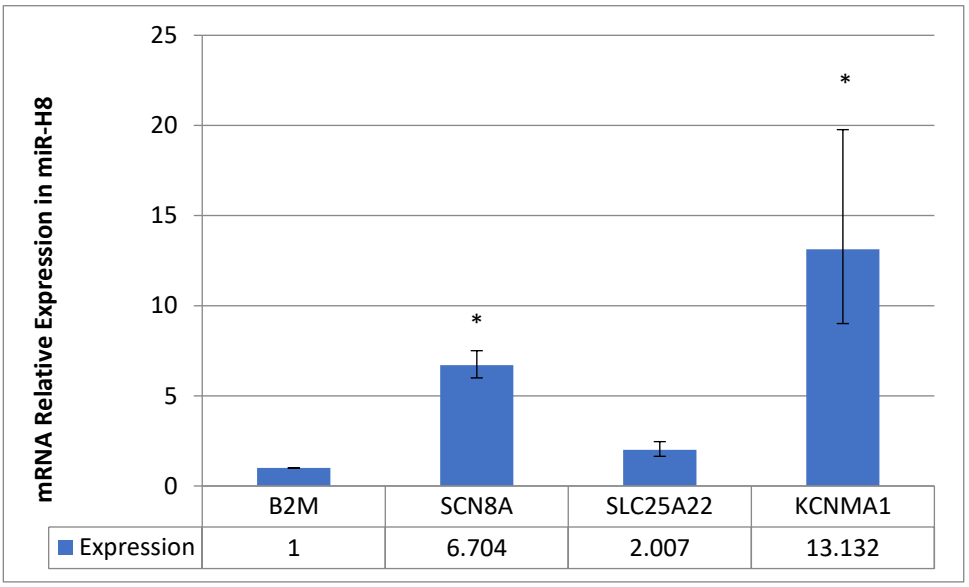

Figure 28. Results of statistical surveys of mRNAs expression data targeted in miR-H8 compared to backbone group (pLenti-III) in HEK293T cells

As figure.28 shows the effect of miR-H8 on the direct target genes of miR-H2 namely SCN8A and SLC25A22 is increasing effect and on the KCNMA1 gene that has been introduced as a direct target of miR-H3, is also increasing effect. In the statistical calculations performed by Rest2009 software, if the p-value is greater than .05 or the expression changes scope exceeds a certain limit, the obtained result is announced as insignificant statistically. For example, although the expression of the SLC22A2 gene affected LAT transcript as shown decrease, but because the p-value is a figure greater than .05, so this result isn't considered significant statistically. The range of genes-related changes has been shown in the diagrams by error bars.

Table 33. Rate of 3'UTR-SLC22A2 expression in HEK293-T transfected cells compared to expression increase of miR-H2 and miR-H3

Group	Firefly (RUL/S)	Renilla (RUL/S)	$\frac{\text{Renilla}}{\text{Firefly}}$	Mean $\frac{\text{Renilla}}{\text{Firefly}}$
C-1	1396427	1563863	1.11	1.01
C-2	1785756	1714627	0.96	
C-3	1774569	1705514	0.96	
miR-H2-1	1197795	1145990	0.95	1.153
miR-H2-2	2021285	2252177	1.114	
miR-H2-3	897028	1238583	1.38	
miR-H3-1	1212417	915616	0.75	0.848
miR-H3-2	830376	918157	1.105	
miR-H3-3	1158940	799942	0.69	

C is the symbol of a control group that here our control group pCDH-CMV-MCS-EF1-cGFP-T2A-Puro has cloned without any piece. In Figures 3 and 30, the expression rate of this gene has been exhibited that has been obtained through reading by Luciferase device.

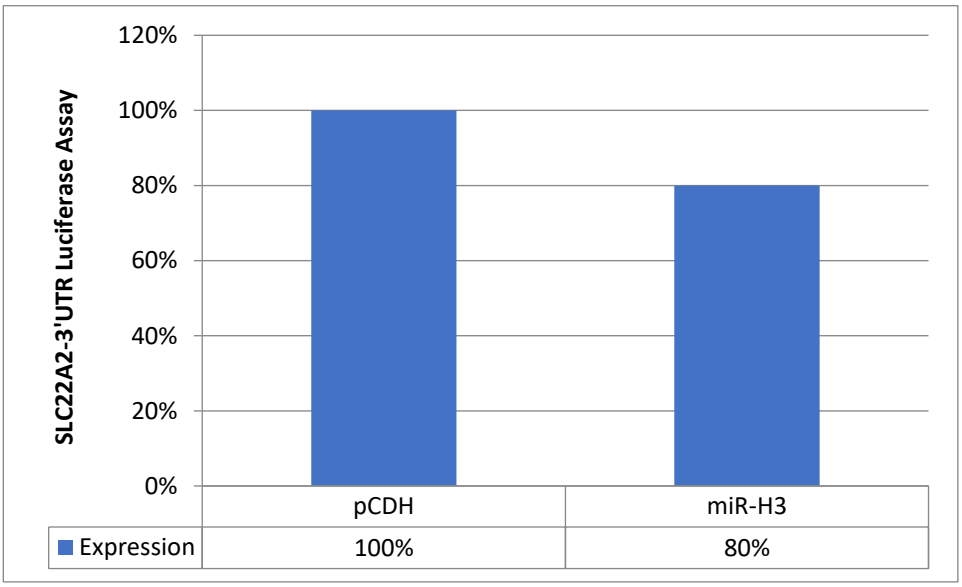

Figure.29. Percentage exhibition of control rate of 3'UTR-SLC22A2 gene expression under miR-H3

The calculation method is such that based on the reagents we add to the transfected cells in the special vial of the device, the number being read will be a representative of the firefly and the second number will be representative of Renilla. Such that by adding the LARII reagent, the activity of the Firefly Luciferase, and then by adding the Stop & GLO reagent, the activity of Renilic Luciferase is determined. Accordingly, we do the same work for all control groups, groups containing miR-H2 and mir-H3. According to Table 29 and the obtained data, only miR-H3 has been able to affect the expression rate of 3'UTR of the concerned gene and in its presence, the SLC22A2 gene has shown only a 20% expression decrease in HEK293T cells and this implies that has been expressed by 80%. While in the presence of miR-H2 that was targeted according to the TargetScan statistical analysis, the expression rate hasn't changed in the presence of this miRNA. Following bioinformatic studies, and detection of the targets of miRNAs in the LAT transcript, and considering the importance and sustainability of H2 and H3 miRs in the conducted studies, these two miRs and their interaction with our target genes were determined as the objectives of the study. In the study of MiR-H2 and miR-H3 at the quantitative polymerase chain reaction level, both of them showed a significant increase in the expression of H2 (about 328 fold) and H3 (136 fold) in HEK cells respectively. The present study is regarded as one of a kind since it investigates the effect of each of these miRs on gene targets that have been analyzed with the software. It can be argued that this is the first attempt to study the effect of viral miRs on the effectiveness of human genes in Iran and other scientific domains.

miR-H2 severely reduces the expression of the SCN8A gene which is an important sodium channel in the central nervous system. According to the results, the quantitative polymerase chain reaction is significantly reduced. The SLC22A2 gene which is an ion carrier from the SLC family is recognized as another target of the miR-H2. The channel was introduced as one of the cancer drug therapy targets due to serving as a passage for a wide range of substances, especially drugs. The role of this gene in epilepsy was discovered in 2017. The diseases associated with this gene and other members of the family are listed in Table (11). The results of real-time PCR on this gene showed a significant reduction in the expression of this gene. Another target of miR-H2 is an ion carrier known as SLC25A22, which, just like the other two genes, proved to have a reductive effect on the real-time PCR reaction. This gene plays a key role in the transition of materials through the cell membrane, and its functional deficiency causes a disturbance in the ion balance within the cell which plays a significant role in the development of diseases of the central nervous system, especially epilepsy. As for miR-H3, although Only one target gene, KCNMA1, has been identified for it, this gene that is a potassium channel (one of the most important and diverse ion channels at cellular levels) plays a very important role in cellular balance, especially in the central nervous system, through the passage of materials, as well as the stimulation of neurons and maintaining their function. Contrary to the results of the analysis performed using Target Scan software and our expectations of KCNMA1 to show a decrease in expression in HEK cells, we observed a 35-fold increase in expression. Of course, these results were obtained after several replications of the qPCR reaction, all of which increased its expression. Since all the herpesvirus miRs originate from the LAT transcript, attempts were made to investigate its effect on our gene targets and also all MiRs found in LAT, because increased expression of KCNMA1 may be because it is targeted by other miRs of the virus, but this has not been discovered in software analyses due to statistical errors. Accordingly, in the next step, all virus miRNAs,

including H2, H3, H4, H5, H7, and H8, and LAT transcript underwent plasmid extraction and were then transfected into HEK293T cells. (At this stage, the pLenti-III-EGFP vector was used). Subsequently, the following qPCR reactions were performed:

Expression of all miRs of the Herpes Virus under the effect LAT Transcript: All miRs in HEK cells showed signs of increased expression, with the highest levels related to H2, H4-5P, and H5-5P (621688, 337209 537455-fold, respectively). Of course, the other miRs, including H3, H7, and H8 also showed signs of increased expression, but the increase in expression of these miRs was much lower compared to others, (6,989,96 and 6,355 / 6 respectively)

2) The expression of other miRs of the Herpes Virus: after H2 and H3, H4-5P, H7, and H8 also showed signs of increased expression (2778, 311.05 and the lowest for H8, 1 345.1, respectively). However, the level of H8 expression under the effect of LAT was slightly higher and had an increasing effect on it. On the contrary, H7, which did not show much expression in LAT, increased expression 300-fold. But others, such as H2, H3, and H4-5P, showed signs of increased expression both collectively and individually, and seem to be powerful miRs compared to the rest. However, the effect of H5 was not investigated separately because of its absence in the expression vector.

3) Evaluation of target genes of ion channels under the effect of LAT transcript: In this study, the expression of SCN8A and SLC22A2 genes decreased by 0.292 and 0.282, respectively. This reduction was repeated when tested with H2 alone. The SLC25A22 gene underwent increased expression (3.655) when tested by LAT, but underwent reduced expression when tested with H2 alone. The KCNMA1 gene, according to the result that was repeated with H3, underwent increased expression by 33.104. In the case of these two genes, there appear to be signaling pathways and upstream and downstream genes that inhibit their expression reduction effects, as expected from statistical analyses. On the other hand, it was assumed that since all of these miRs originate from the LAT transcript, the reduction in gene expression is supposed to have a down-regulating effect when tested by both miR and LAT.

4) Evaluation of target genes of ion channels under the influence of other viral miRs. In this study, we managed to evaluate SCN8A, SLC25A22, and KCNMA1 genes with all herpes miRs (except for miR-H5). The results are provided below:

1) The previous results obtained with H2 for SCN8A and SLC25A22 genes were also consistent in the final replication and showed reduced expression (0.01 and 0.93, respectively). It seems that these two genes are strongly suppressed by H2. The KCNMA1 gene experienced reduced expression (0.883), which according to REST software analysis, was not significant.

2) SCN8A, SLC25A22, and KCNMA1 genes showed increased expression in the H3 test, (5.818, 3.138, and 24.847 respectively)

3) SCN8A, SLC25A22, and KCNMA1 genes showed increased expression in the H4 test (11.236, 12.084 and 31.183, respectively)

4) SCN8A, SLC25A22 and KCNMA1 genes showed increased expression in the H7 test (570.45, 2.302 and 10.111, respectively)

5) SCN8A, SLC25A22, and KCNMA1 genes showed increased expression in the H8 test (6.704, 2.007, and 13.132, respectively) (however no significant increase was observed for SLC25A22). The overall conclusion of the data shows that the SCN8A gene is suppressed by its target miR, H2, and the LAT transcript, and although it has undergone increased expression by other viral miRs, it seems that the suppressing power of H2 In the LAT transcript has been dominant. The expression of the SLC25A22 gene has been suppressed by miR-H2 but has been increased by other miRs and LATs. It seems that other miRs may have targeted it, and other unspecified genes have been involved in the increased expression of this gene. This analysis also holds for KCNMA1. After obtaining the aforementioned results, attempts were made to clone the genes to determine the extent to which the genes in question were reduced in the cell so that the gene would be directly transfected into HEK cells and its effect can be investigated using miRs. using the available facilities and the suitable enzymes for cloning, we managed to clone a SLC22A2 gene, which had a shorter 3'UTR fragment, into a psiCHECK vector, and then transfect it into the cell along with H2 and H3 miRs. Analysis of the Luciferase results showed that the expression of the gene was reduced by miR-H3 alone and that this gene is expressed by 80% in HEK293T cells, this means that miR-H3 has managed to suppress the gene expression by 20%. While miR-H2 has not had any effect on the reduction of gene expression. This is completely inconsistent with the results of qPCR. On the other hand, the role of LAT has been ignored in the present study, and, to obtain more accurate results, it is necessary to repeat the test in the presence of a LAT transcript.

It is also necessary to repeat this test with other viral miRs, to ensure accurate results in terms of this effect. The role of the LAT transcript in the determination of the host cell fate, as well as its effect on host factors and genes that contribute to infection, served as a motive for the conduction of the present study. Identification of new targets for these viral miRNAs not only helped us get to know about the mechanisms associated with infection and latency of the HSV-1 virus but can play an effective role in the clarification of the rest of the mechanisms

associated with the employment of the virus in the nervous system and developing useful therapeutic approaches for the diseases associated with it. it should be noted, however, that epilepsy is only one of the examples of herpes infection and traces of this virus has been seen in other diseases of the central nervous system such as Alzheimer's disease, Parkinson's disease, glioblastoma, and other nervous and neurological disorders. The most important achievement of this plan is the contribution to the identification of the Molecular causes as well as the pathways that contribute to the exploitation of the host environment by the virus. This achievement could significantly contribute to the colonization of the herpes virus and even its latency effect until the end of human life without causing any infection. Moreover, the present study could lead to a major development in the treatment approaches as well as the improvement and development of medications. It should be noted that the effect of herpes miRs, with behavior similar to that of human miRs, on host gene targets was investigated for the first time in the present study.

Conclusion

The HSV-1 can use its miRNAs, such as human miRs, to control the expression of ion channels, such as SCN8A, SLC22A2, SLC25A22, and KCNMA1. Using the Target Scan software, the possibility of targeting the ion channel genes originally mentioned was investigated for each of the LAT miRs, followed by two miRs for continued laboratory work. After building up gene constructs containing each of the miRs and their transfection into the HEK293T cell line, increasing the expression of miRs was confirmed by the Real-Time PCR technique, as well as increasing the expression of each miR. The production of LAT-infected plasmid transfected plasmid containing LAT and miRNAs of H4-5P, H5-5, H7, and H8 was each measured individually. We first examined the expression of the genes separately with H2 and H3 miRs with Real-time PCR reaction. In order to see the effect of LAT transcription on any of the genes, we conducted the timing reaction on the cDNAs that were made by LAT transcription into HEK293T cells. Also, the Luciferase test has been done for one of the genes, SLC22A2. The outcome of these studies was to reduce the expression of SLC22A2 and SCN8A genes both in the study with miR-H2 and in the review with LAT. The Luciferase assay showed that SLC22A2 was suppressed only by miR-H3, which should also be checked for confirmation of the effect of LAT transcript. The collections examined by these channels are all part of the genes involved in neurological diseases, and in particular epilepsy. Ionic channels can be involved in epilepsy due to mutation or functional impairment, in which the SCN8A sodium channel plays a major role in these disorders. However, the role of other channels, including KCNMA1 and SLC25A22 can be considered.

Acknowledgment:

The authors would like to express their gratitude to"Bonyakhteh" comprehensive stem cell biology and regenerative medicine center for their support and contribution to this study .

Conflict of Interest:

All authors hereby declare no conflict of interest.

Funding:

This work was funded by University of Tehran, college of microbiology.

References

[1] Ryan KJ, Ray CG (editors) (2004). Sherris Medical Microbiology (4th ed.). McGraw Hill. pp. 555–62.

[2] Eulalio, A., F. Tritschler, and E. Izaurralde, The GW182 protein family in animal cells: new insights into domains required for miRNA-mediated gene silencing. Rna, 2009. 15(8): p. 1433-1442.

[3] Schiffer JT, Mayer BT, Fong Y, Swan DA, Wald A (2014). "Herpes simplex virus-2 transmission probability estimates based on the quantity of viral shedding". J R Soc Interface. 11 (95): 20140160.

[4] Sperling RS, Fife KH, Warren TJ, Dix LP, Brennan CA (2008). "The effect of daily valacyclovir suppression on herpes simplex virus type 2 viral shedding in HSV-2 seropositive subjects without a history of genital herpes". Sex Transm Dis. 35 (3): 286–90.

[5] Gottwein, E., X. Cai, and B. Cullen. Expression and function of microRNAs encoded by Kaposi's sarcoma-associated herpesvirus. in Cold Spring Harbor symposia on quantitative biology. 2006. Cold Spring Harbor Laboratory Press.

[6] Lo, A.K.F., et al., Modulation of LMP1 protein expression by EBV-encoded microRNAs. Proceedings of the National Academy of Sciences, 2007. 104(41): p. 16164-16169.

[7] Grey, F., L. Hook, and J. Nelson, The functions of herpesvirus-encoded microRNAs. Medical microbiology and immunology, 2008. 197(2): p. 261-267.

[8]Zabolotny, J.M., C. Krummenacher, and N.W. Fraser, The herpes simplex virus type 1 2.0-kilobase latency-associated transcript is a stable intron that branches at guanosine. Journal of Virology, 1997. 71(6): p. 4199-4208.

[9] Zhou, M.-Y .and C.E. Gomez-Sanchez, Universal TA cloning. Current issues in molecular biology, 2000. 2: p. 1-8.

[10] Isom, L.L., et al., Primary Structure and Functional Expression of the \beta_1 Subunit of the Rat Brain Sodium Channel. Science, 1992: p. 839-842.

[11] Ogata, N. and Y. Ohishi, Molecular diversity of structure and function of the voltage-gated Na+ channels. The Japanese Journal of Pharmacology, 2002. 88(4): p. 365-377.

[12]Doyle v. Wallace, in PIQR Q. 1998. p. 146.
[13] Shieh, C.-C., et al., Potassium channels: molecular defects, diseases, and therapeutic opportunities. Pharmacological reviews, 2000. 52(4): p. 557-594.
[14]Hediger, M.A., et al., The ABCs of membrane transporters in health and disease (SLC series :(introduction. Molecular aspects of medicine, 2013. 34(2): p. 95-107.
[15] Haitina, T., et al., Fourteen novel human members of mitochondrial solute carrier family 25 (SLC25) widely expressed in the central nervous system. Genomics, 2006. 88(6): p. 779-7.90